Experimental Investigation of Bubble Formation in Micro-devices

Nicolas Dietrich, Souhila Poncin, Huai-Zhi Li

Experimental Investigation of Bubble Formation in Micro-devices

N. Dietrich, S. Poncin & Huai Z. Li
Laboratoire des Sciences du Génie Chimique, Nancy-Université, CNRS, 1 rue Grandville, BP 20451, 54000 Nancy Cedex, France. Tel +33 0383175367 E-mail: Dietrich@ensic.inpl-nancy.fr

Keywords: bubble formation, micromixer, flow focusing, correlation, μ-PIV

Abstract

The multiphase flows (gas-liquid-solid) in Newtonian and non-Newtonian fluids are involved in many industrial processes. Among these processes we can mention polymer devolatization, bubble columns, cosmetics, petrochemical, water treatment and bioprocesses. These systems are generally accompanied by heat and mass transfer as well as chemical reactions. In this context, the effectiveness of the heat and mass transfers is a main parameter that depends primarily on the nature of the gas-liquid or solid-liquid interfaces. In addition, some reactions, such as the fluorination of toluene are very dangerous and difficult to achieve at a large scale. Thus the realization of this kind of reactions in microsystems is much more safe and effective.

That is why over the past few years, many studies (van Batten *et al.*, 2004) and Garstecki *et al.*, 2006) focused on the application of these processes at smaller scales, ranging from one hundred micrometers to a millimeter, leading to the emergence of gas-liquid micro-reactors. In the past, several studies have been focused on certain aspects of these flows, particularly the exchange of mass and pressure differences, but most of these studies are numerical and very few experimental studies have been conducted yet.

The objective of this study is to compare micromixers of different sizes (channel size of 500, 800 and 1000 μm) and geometries (Y-junction, T-junction, cross section). In order to understand the mechanism of bubble formation, different gas and liquid flow rates, liquid viscosities and surface tensions were used. A High speed camera (10 000 images/second) and also a system of micro-Particle Image Velocimetry (μ-PIV) were also used to measure the velocity flow field at micro-scale as shown in Figure 1. A correlation is proposed to estimate the bubble size for the different micromixers. This paper contributes to an original improvement in the domain where a few flow field characterisation and micro mixers comparisons have been published in the literature.

1. Introduction

Multiphase flows in microfluidic devices have received more attention because of the foreseeable advantages that unique microscale properties have to offer with regard to enhanced heat and mass transfer efficiency, reduced axial dispersion and smaller sample volumes. In order to realize these benefits, a good understanding of the complex multiphase flow behavior in microfluidic devices must be developed. Formation of bubbles serves various applications in industrial processes such as the generation of biogas bubbles by anaerobic sludge granules in a bioreactor (Wu *et al.*, 2006), bubble nucleation in polymer devolatization processes (Frank *et al.*, 2007), two-phase micro-mixing (Garstecki *et al.*, 2006), fluorinations (Chambers *et al.*, 2001), hydrogenations (Kobayashi *et al.*, 2004), biochemical reactions such as DNA analysis (Burns *et al.*, 1998), micro-channel heat

exchangers (Qu and Mudawar, 2002), materials synthesis (Yen *et al*., 2005; Zhang *et al*., 2006), drug discovery (Dittrich and Manz, 2006).

The two-phase flow patterns in microchannels are determined by the flow conditions, the channel geometry and the properties of both fluids (Waelchli and Rohr, 2006). The bubbly flow is characterized by the formation of single spherical bubbles with bubble lengths smaller than, or equal to the channel width. Increasing the gas flow rate causes the coalescence of small bubbles leading to cylindrical bubbles (separated from the wall by a thin film), this regime is known as slug. Generally, bubbly flow appears at high liquid velocities and low gas velocities and slug flow occurs at intermediate gas and liquid velocities while annular flow appears usually at high gas velocities. In this study experiments are mainly focused on the segmented gas-liquid flows, i.e., bubbly and slug regimes.

The most popular geometries for the production of dispersed phases are T-junctions (Garstecki *et al*., 2006; van der Graaf *et al*., 2006; Guillot and Colin, 2005; Nisisako *et al*., 2002; Thorsen *et al*., 2001; Tice *et al*., 2003; Xu *et al*., 2006) and flow-focusing devices (Anna *et al*., 2003; Cubaud *et al*., 2005; Ganan–Calvo and Gordillo, 2001; Garstecki *et al*., 2005). Garstecki, *et al*. (2005) used the flow focusing device with a small orifice to generate monodispersed bubbles. They found that the bubble formation was due to the pressure gradient and the breakup could be controlled by the flow rate of the continuous liquid phase. Cubaud and Ho (2004) studied the formation of bubbles in square micro-channels. The bubbles were generated in a cross-shaped mixing section. Theses authors reported that the breakup mechanism in their device could be understood as the competition between the pressure drops respectively in the gas and liquid phases.

In order to gain more insight into the bubble breakup in such microfluidics devices, liquid flow field velocities were investigated using μ-PIV techniques. The μ-PIV technique was successfully used to characterize single-phase flow in microfluidic T-junctions (Lindken *et al*., 2006) and segmented multiphase flows in labs-on-chips. The μ-PIV studies in literature mainly deal with the flow or the formation in one channel and very few papers are devoted to the velocity flow field at a bubble formation. Velocity fields obtained by μ-PIV at bubble formation were reported for a T-junction (Van Steijn *et al.,* 2007) and for a Y-junction (Dietrich *et al.,* 2007) but it is not the case for the flow focusing micro-mixer to our best knowledge.

For many industrial applications, it is essential that one can predict the geometric features of the flow pattern, such as bubble and slug length. In several studies, correlations have been proposed to determine the characteristics of the bubble (length or volume). Ganan-Calvo (1998) proposed a correlation for jet flows; Ganan-Calvo and Gordillo (2001) studied a cross flow focusing mixer and proposed a correlation between the bubble length and flow rate ratios without including physical properties. Cubaud *et al.* (2005) showed that the length of the produced confined bubbles follows a law based on the channel size and the liquid volume fraction. Garstecki *et al*. (2006) studied a cross flow micro-mixer and also developed a simple correlation between flow rates ratios and the length of the bubble. To our knowledge, no correlation based on the bubble volume or on the physical properties of the liquid phase has been proposed and the existing correlations have always been based on only one geometry of micro-mixer.

The effect of the micromixer geometry was investigated by Haverkamp *et al.* (2006). The authors designed two mixing geometries, namely, the "T-type" and the "smooth" mixers and studied the flow of gas-water in both mixers. They reported that the breakup by pressure gradient was only observed in the T-type mixer, while the jet instability was the only mechanism for bubble formation in the smooth mixer. Fan *et al.* (2007) studied two types of mixer geometries including the cross-shape and the converging shape channels. The bubble shape and size and the formation mechanism were investigated for different flow rates and

different mixer geometries. Theses authors compared simulated results with experimental data based on dimensionless numbers. A good agreement was found in general. Different flow regimes with different bubble shapes were found depending on the capillary number of the flow. The simulation confirmed that the breakup was induced by the pressure difference in both phases. The geometry of the mixing section was also observed to have an impact on the size of the gas and liquid slugs, but no experimental quantification of bubble size and velocity flow field has been done. The present paper is focused on the formation of bubbles in flow-focusing micro-reactors of different geometries. Since the most important forces in multiphase flows are the inertial force, viscous force and interfacial force, the goal of our study is to understand the importance of theses forces for different reactor geometries in order to give more insight into then bubble formation in flow focusing micro-mixers. A µ-PIV system and a high speed microscopic camera were employed for these reactors leading to new features in this domain.

2. Experimental setup

The different geometries of microfluidics devices used in this study are reported in Figure 1. The micro-channels were fabricated in polymethyl methacrylate (PMMA). This flow-focusing geometry had a central channel for the gas dispersed phase flow and two side channels for the inlet of the continuous liquid phase. Two sizes of liquid inlet and outlet channels (600 µm and 1000 µm) and of gas inlet channels (200 µm and 500µm) were used. The section of the gas inlet was circular in order to avoid wetting problems, the other sections being square to assure a better view of the flow field.

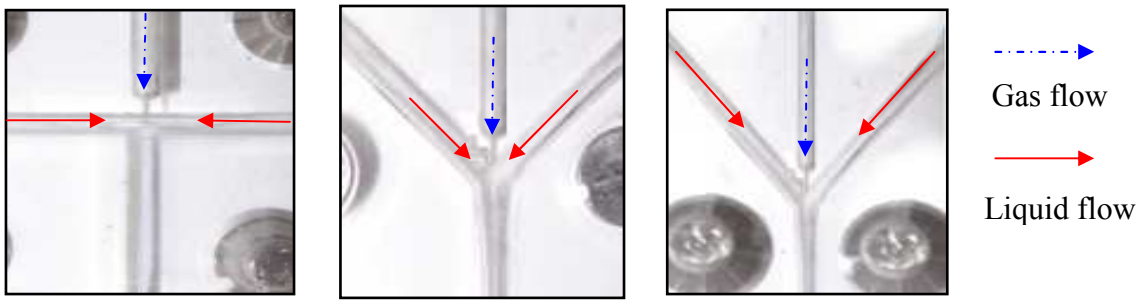

***Figure 1**. Illustration of the micro fluidic chip used to generate micro bubble. From the left to the right, cross shape (180°), Convergence shape (90° and 60°).*

A pressurized tank of 10^{-3} m^3 was used to maintain a constant pressure and to push the liquid and air streams into the micro-channel with a regular flow rate of both phases. A gas flow-meter is used to determine the flow rate with precision. Images of bubbles were captured at steady state on the high speed camera CamRecord600 from Optronis GMBH (Kehl, Germany), capable of 500 frames per second at full resolution (1280×1024) with a microscopic objective ranging from × 100 to × 600. The length of the bubble was determined by an image analysis software and the volume of the bubble was calculated from the gas flow rate and the bubble formation frequency determined by the high speed camera as follows:

$$v_b = \frac{Q_g}{f_{formation}} \qquad (1)$$

The Instantaneous liquid velocity flow fields were measured by a µ-PIV of DANTEC Dynamics (Skovlunde, Danemark). The system consisted of a Flowsense Dantec Camera with a 2048×2048 pixel array and a 7 Hz frequency. The microscope was equipped with different objectives ranging from ×5 to ×100. The micro-device under investigation faced the microscope and was illuminated from the back by a micro-strobe emitting at 530×10^{-9} m.

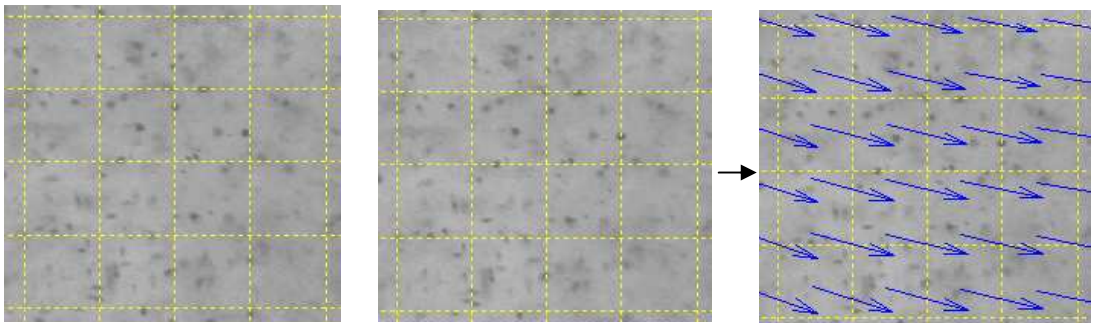

Figure 2. *Micro Particle Image Velocimetry principle (µ-PIV). 50×50 µm windows.*

The liquid velocity was measured by imaging (and evaluating) the motion of seeding particles suspended in the fluid. The principle of PIV is reported in Figure 2. The camera takes two successive images at the maximum intensity of the micro stroboscope impulse. The acquired images of the flow are evaluated by dividing the images into a few thousands of small interrogation areas of 16×16 pixels. A cross-correlation is then applied on the interrogation areas in consecutive images with a 50% window overlap. For each interrogation area, the displacement vector is calculated from the location of the correlation peak. The velocity field is then calculated from the displacement vectors and the time chosen between the images. The depth of field of the microscope is between 10 and 40 µm, which means that measurements are not realized on a plane but on a slice of the micromixer. However, this value is negligible in comparison with the thickness of the microchannel. To obtain velocity flow fields, the tracer particles must perfectly follow the flow. Seeding should be uniform and at a reasonable concentration. The density should be similar to the studied fluid. If the tracer used is made of too small particles, Brownian motion (Robert Brown, 1927) can influence the measurements. This random motion of particles sets a lower limit to achieve µ-PIV measurements. Starting from the equation of Einstein-Sutherland (1905), one can estimate the influence of this Brownian motion. Equation 2 establishes the relationship between the diffusion coefficients of a colloid D and colloid properties.

$$D = \frac{kT}{6\pi\mu r} \qquad (2)$$

T is the temperature, µ the viscosity of the fluid, r is the radius of the particle and k the Boltzmann constant. This equation shows that more the radius of the particle is low more the Brownian motion is great. The standard deviation of the random movement of a particle is given by equation 3:

$$\Sigma_p = \Delta x_p \approx \sqrt{2D\delta t} \qquad (3)$$

Thus, for a camera acquisition frequency of 4 s^{-1} and a particle diameter of 200×10^{-9} m, the random movement is estimated at 3×10^{-6} $m.s^{-1}$. The values of the liquid velocity used in this study being of about a few hundred µm per second, one gets an error of several percent on the velocity estimation. We must therefore focus on larger particles to avoid problems due to Brownian motion. But bigger the particle is, bigger is its settling velocity. The sedimentation velocity of a particle diameter d is estimated as follows:

$$V_p = \frac{d^2 g(\rho_g - \rho_p)}{18\mu} \quad (4)$$

For seeding particles of 3×10^{-6} m, the value of the sedimentation velocity becomes of the order of 1.5×10^{-6} m per second. Finally to contain the contribution of both Brownian motion and settling velocity less than 1% of the measured velocity, the optimal size of seeding particle has to be in the range [0.5-3×10^{-6} m]. Furthermore, the size of the geometry, viewing windows and objectives also will help to refine the value of the particle diameter. In this study, hydrophilic latex microspheres (Merck Estapor, Fontenay sous Bois, France) with a density of 1056 kg.m^{-3} and a mean diameter calibrated of 0.88×10^{-6} m were used as seeding particles. These particles were small enough to follow the fluid and large enough to avoid the Brownian motion effects. When the flow is correctly inseminated, the measurement errors of the measured velocities are less than 5%.

In this work, the experiments were performed using air as gas phase and three different liquids (pure water, viscous Newtonian Emkarox HV45 10% and 20% wt dilute solutions in demineralised water). A Rheometric Fluid Spectrometer RFS II (Rheometric Scientific) was employed to measure the rheological properties of the liquids (Table 1). The surface tensions and the contact angle of the liquid on PMMA surface were measured using a tensiometer, by the pending drop technique on a Tracker apparatus from I.T. Concept (Longessaigne, France). Sodium Dodecyl Sulphate surfactant (SDS, Amersco, USA) was also used to control the tension force, which allows to compare separately the effect of tension force and viscosity. Table 1 lists all properties of the various liquids used. All experiments were carried out at a constant temperature of 293K.

Table 1. *Properties of the different liquids used in this study at 293K.*

Fluid	ρ *(kg.m^{-3})*	μ *(×10^{-3} Pa.s)*	σ *(×10^{-3} N.m^{-1})*
Water	1000	1	72
Water + 0.10% SDS (wt)	1000	1	50
Water + 0.15% SDS (wt)	1000	1	40
HV45 10% (wt)	1030	10	50
HV45 10% (wt) + 0.05% SDS (wt)	1030	10	40
HV45 25% (wt)	1050	30	40

3. Experimental results

In this work, experimental results of the bubble formation obtained in three different micro-mixer geometries (180, 90 and 60°) are presented. In order to understand the key parameter of the bubble formation process, a preliminary study was realized to understand the influence of each factor. The gas and liquid flow rates ranged from 10^{-12} m^3 s^{-1} to 10^{-6} m^3 s^{-1}, which corresponded to bubbly and slug flow regimes and bubble diameters between 50×10^{-6} m and 5×10^{-3} m. Our first contribution in this work is to characterize the bubble formation using µ-PIV and high speed camera images. The evolution of the bubble shape at different time during the formation process of a 10^{-9} m^3 bubble growth up to its detachment is shown in Fig. 3. The flow was highly periodic with a bubble frequency of 34 s^{-1}. Figure 3 shows the growth process during one period. The bubble shapes were obtained from a high speed camera images. One can distinguish three steps during the formation of the bubble: a first rapid expansion step of the growing bubble, followed by a linear increase of the bubble during the second step, and finally the last step corresponds to a very quick elongation of the bubble which is stretched from the orifice and elongated due to the lateral flow leading to its rupture.

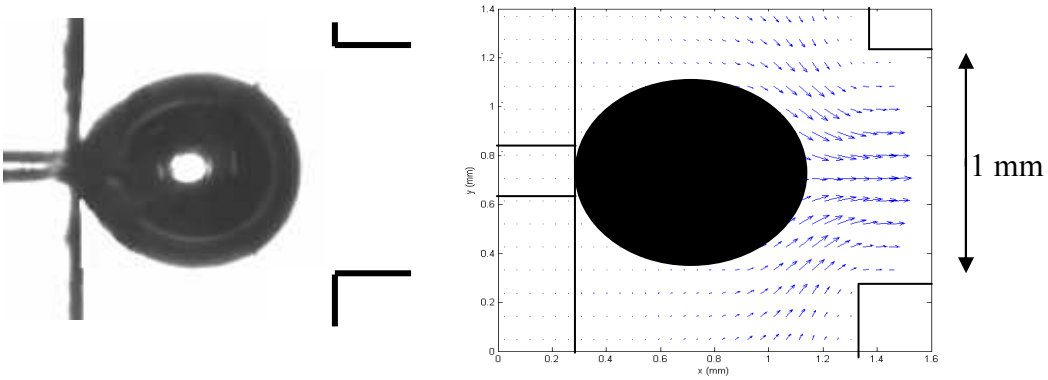

Figure 3. *Formation of micro bubbles in water. On the left: formation of a bubble in a cross flow focusing microreactor (channel size inlet 200 µm and outlet 1000 µm) using a high speed camera (1024*1280 pixels, 1000 Hz). On the right, the velocity field obtained with a µ-PIV system (2048*2048 pixels, 7 Hz) using seeding particles of 0.88 µm.* V_{bubble} *=* $1.14\ 10^{-9}\ m^3$. $Q_{liquide} = 10^{-7}\ m^3/s$. $Q_{gas} = 10^{-8}\ m^3/s$. $t_{formation}$ *= 26 ms*

Obviously, bubbles expand spherically at the beginning of the bubble formation, then evolved from spherical shape to symmetrical teardrop shape. In this stage the bubble grows without significant movement into the stream direction and the liquid flows easily around the growing bubble. Subsequently, the effect of flow inertia on the bubble becomes gradually important during the growth of the bubble, the interface moves and the bubble is stretched forming a neck that is elongated to an obvious teardrop shape up to the rupture.

The µ-PIV technique is a powerful tool to evaluate the main forces acting on the bubble interface during the formation. Fig. 3 represents the velocity fields around a forming bubble in a cross shape flow focusing micro-mixer.. As shown in this figure, the neck interface undergoes shearing which can be estimated from the parallel liquid velocities at the interface of the bubble. In examples presented in Figure 3, the shear rate is about 500 s^{-1}. But, by evaluating the others pressure drop force acting on the bubble shows that, the shear is not the key force. The main mechanism depends on the competition between several different forces. Formation is due to a balance between static pressures forces and tension force. The measurement of the flow field around a bubble in formation in a flow focusing microfluidic systems comforts the literature results (Cubaud *et al.,* 2005 and *Garstescki et al.,* 2006) about the physical formation mechanism. Moreover, as shown in Figure 3, the bubble shape is not so deformed. This can be explained from the values of the pressure drop at the bubble formation and that of the interfacial pressure defined by the Laplace-Young law. The interfacial pressure estimated for the case presented in Figure 3 is quite high aroundt 483 Pa, which results in a very small deformation of the forming bubble. In addition to the measurement of local flow properties by means of µ-PIV, the global properties such as bubble length or volume were measured using a high speed camera and a flowmeter. It is therefore possible to determine the physical key factors involved in the formation mechanism.

The flow rate ratio seems to have an important influence on the formation of micro-bubbles. Figure 4a presents the evolution of the dimensionless ratio L/W of the bubble length to the channel width with the gas flow rate (when liquid flow is constant) and inversely.

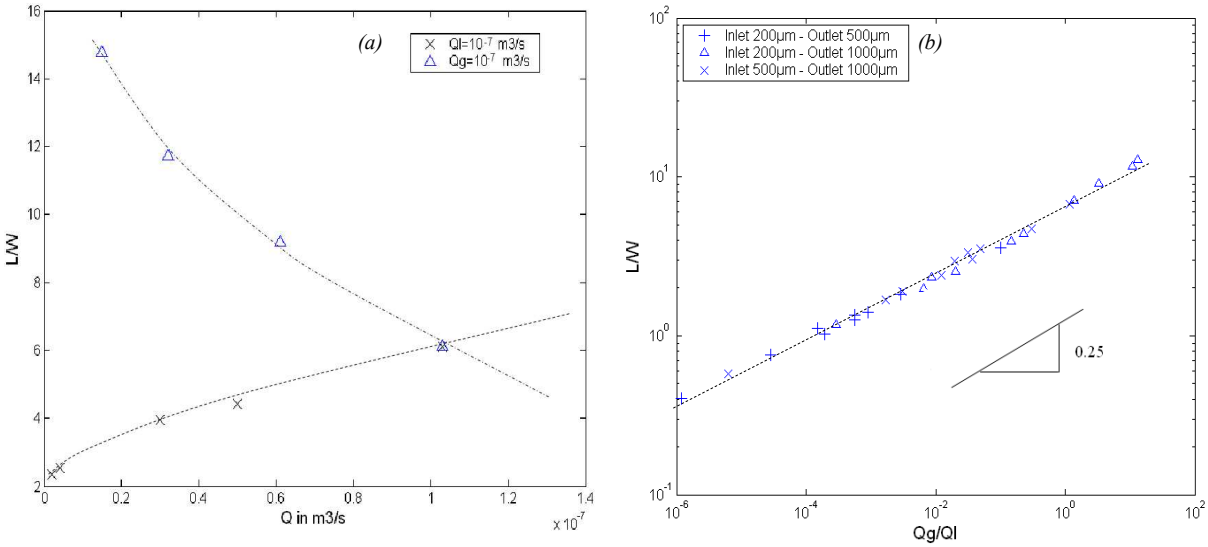

Figure 4. *(a) Influence of gas or liquid flow rate on the bubble length to channel width ratio (L/W). (×) versus Q_g at constant Q_l (△) versus Q_l at constant Q_g .Inlet channel size 200µm and outlet channel size 1000 µm.(b) Effect of inlet and outlet channel sizes on the evolution of L/W as function of the flow rate ratios in water.*

These results show that the detached bubble length is affected by both gas and liquid flow rates. The bubble volume gradually increases with the gas flow rate, and decreases with the liquid flow rate. This slow evolution may be explained by the increase of shear stress and elongation when the liquid flow rate increases leading to the formation of smaller bubbles. The evolution of L/W ratio as a function of the Q_{gas}/Q_{liquid} ratio for various sizes of gas inlet and gas-liquid outlet (Figure 4b) may be represented by the following correlation:

$$\frac{L}{W} = \beta \left(\frac{Q_{gas}}{Q_{liquid}} \right)^{\alpha} \qquad (5)$$

where $\alpha = 0.25$ is the power index and constant β value depends on the liquid physical properties and the geometry of the micro-mixers. This correlation describes well the influence of both flow rate and also the size of the micro-mixer channels. Furthermore, Eq. 5 is in agreement with that proposed by Ganan and Gordillo (2001), who found a power factor α of 0.37 instead of 0.25 for this study. This is probably due to the wall effects occurring in their micro-channel of which the inlet channel is bigger. In order to improve this equation, the liquid physical properties such as the surface tension σ, the viscosity μ and also the geometry of the mixer were varied to investigate their influence. Figure 5 shows the evolution of L/W ratio as a function of the Q_g/Q_l flow rate ratio.

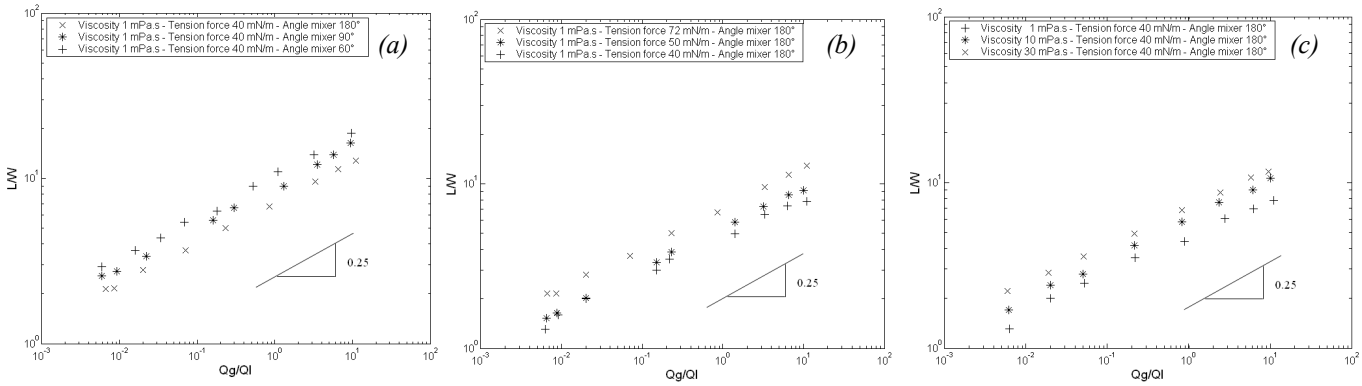

Figure 5. *Influence of the liquid physical properties and micro-mixer geometry. Inlet of 200 µm and outlet of 1000 µm. (a) Influence of junction angle mixer θ_{mixer}. (b) Influence of Tension force. (c) Influence of viscosity.*

One can observe for all the studied geometries, the same tendency of curves reported in Figures 5a, 5b and 5c with the same power index $\alpha = 0.25$. The effect of the mixing section geometry on the bubble length was studied for three types of mixers as shown in Figure 5a: a cross-shaped mixer for which the liquid inlet channel was perpendicular to the outlet channel. The two other types were the converging mixers, with angles of 45° and 30° between both liquid inlet channels and the central gas-liquid outlet channel.

The width of the channels in these geometries was 200 µm for the gas inlet and 1000 µm for the liquid inlet. Experiments were carried out for each geometry using different operating conditions. For the same geometry, increasing the ratio of gas flow rate to liquid flow rate yielded an increase in the bubble length. However, the bubble size increases when the angle θ decreases. The effect of surface tension was investigated using the SDS surfactant in water in one micromixers geometry (180°).

As expected the bubble length is affected by the surface tension and increases with the surface tension (Figure 5b). Finally the effect of the liquid viscosity was investigated in the 180° angle micro-mixer using three liquids of the same surface tension, which was obtained by SDS surfactant addition, as showed in Figure 6c. Once again, the bubble length normally increases with the liquid viscosity which is due to the flattened liquid velocity profiles and to the enhanced shear obtained with higher liquid viscosities.

The β factor presented in Eq. 5 seems to be linked to these three parameters. A dimensional analysis was applied to obtain a dimensionless correlation equation of bubble length for all operating conditions and mixer geometries investigated in this study. For this purpose, 150 data were used to determine such correlation. Table 3 presents the correlations obtained for each mixer geometry. Dimensionless numbers based on viscosity and surface tension were introduced using the physical properties of water μ_{ref} and σ_{ref} as reference.

A good agreement is obtained between measured and correlated values with an average relative error below 3% and a maximum error of less than 13%.

Table 2. Comparison of correlations proposed for the studied micro mixers

θ=60°	θ=90°	θ=180°
$\beta = 10.3\left(\frac{\sigma}{\sigma_{ref}}\right)^{\frac{6}{5}}\left(\frac{\mu}{\mu_{ref}}\right)^{\frac{1}{15}}$ (6)	$\beta = 9\left(\frac{\sigma}{\sigma_{ref}}\right)\left(\frac{\mu}{\mu_{ref}}\right)^{\frac{1}{10}}$ (7)	$\beta = 7.08\left(\frac{\sigma}{\sigma_{ref}}\right)^{\frac{3}{4}}\left(\frac{\mu}{\mu_{ref}}\right)^{\frac{1}{8}}$ (8)
ε = 2.64% error (max 10%)	ε = 3% error (max 12%)	ε = 2.75% error (max 13%)

Two conclusions can be therefore drawn. Firstly, the influence of surface tension is more important than the viscosity, as shear stress is smaller than surface tension pressure. Secondly, the influence of surface tension fincreases when θ decreases (i.e. elongation effect increases) contrarily to the effect of viscosity which increases with θ (i.e. with increasing shear stress). According to Eq. 6, 7 and 8, the viscosity has a bigger influence (1/8 > 1/5) on high angle geometries (for which higher shear stress is obtained) and surface tension has a bigger influence (6/5 >3/4) on small angle geometries (for which higher elongation and formation angle are observed). The effect of surface tension is bigger in smaller angle geometries which confirms once again the effect of interfacial force obtained in correlation of Table 2. Thus μ-PIV measurements can provide useful information in order to validate the correlations established for the studied mixers. In order to take into account the influence of the mixer angle on the behavior induced by the effect of the liquid viscosity and surface tension, a θ/θ_{max} parameter was added in the correlation of Table 3 where θ_{max} is the maximal angle (*i.e.* 180°). The following dimensionless correlation (Eq 9.) was thus obtained which was based on about 150 experimental data.

$$\frac{L}{W} = 8{,}3\left(\frac{\theta}{\theta_{max}}\right)^{-\frac{1}{8}}\left(\frac{\sigma}{\sigma_{ref}}\right)\left(\frac{\mu}{\mu_{ref}}\right)^{\frac{1}{10}}\left(\frac{Q_{gas}}{Q_{liquid}}\right)^{\frac{1}{4}} \quad (9)$$

Figure 6 shows the good agreement obtained between experimental L/W values and those estimated from equation 14.

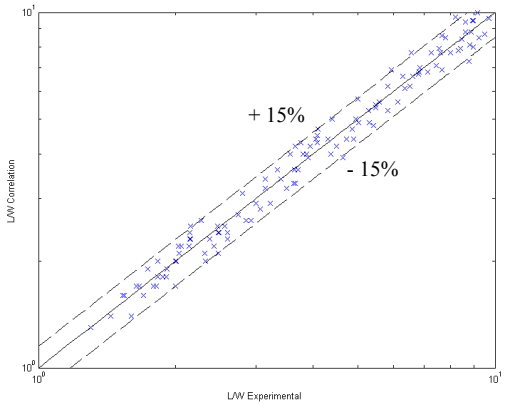

Figure 6. *Parity diagram between correlated data and experimental results.*

The average relative error is about 6.5% with a maximum error of 18.7%. Quite good results are obtained from this correlation for bubble formation in liquid of viscosity ranging from 1 to 30 mPa.s, surface tension of 40 to 72.5 mN/m, and different geometries and size of micro-mixers (angle of 180, 90 and 60° and W = 200, 500 and 1000 μm). It could be a useful tool for micro-reactor design to take into account the liquid physical properties as well as the geometry of the micro-mixers.

4. Conclusion

In this work, experiments were carried out to study the gas-liquid flows in microchannels. The segmented flow of a train of bubbles is important in many applications of multiphase flow in microfluidic devices. The bubble shape, size and formation mechanism were investigated under different operating conditions. The mechanism of bubble formation in a flow focusing micro-mixer was described previously (Garstecki *et al*., 2006; Cubaud *et al*., 2005); the bubbles were usually pinched off by the pressure difference in both phases. The current work confirms the general mechanism of bubble formation by the mean of μ-PIV measurements. The liquid flow field of the continuous phase during the formation of bubbles provides important quantitative details and more insight into the bubble length which was never reported in literature for this type of micro-mixer. Moreover, bubble size was shown to depend on the liquid physical properties (viscosity and surface tension) and the geometries of the mixing section. In regard to a different mixer, the viscosity and the surface tension have variable influence. Finally, the correlations were proposed to predict the bubble volume and length for all gas-liquid systems and micro-mixer geometries investigated and a good agreement was observed between experimental results and predicted values.

Notation

V_b *bubble volume, m^3*
W *Channel width, m*
θ *Angle , °*
Q *Flow rate, m^3s^{-1}*
L *Length, m*
r *Radius, m*
k *Boltzmann constant, J/K*
D *Diffusion coefficient, m^2/s*
T *Temperature, K*
V *Velocity, m/s*

Greek Letters

$\dot{\gamma}$ *Shear stress, s^{-1}*
ρ *Density, $kg.m^{-3}$*
μ *Viscosity of the liquid , Pa.s*
σ *Tension force, $N.m^{-1}$*
α, β *Power law coefficient*
Σ *Standard deviation, m*

Subscripts

$_g$ *Gas*
$_l$ *liquid*
$_p$ *Particle*
$_{ref}$ *Reference properties*
$_{max}$ *Maximal*

Literature Cited

Anna, S.L., Bontoux, N., and Stone, H.A., 2003. Formation of dispersions using ‘‘flow focusing’’ in microchannels. Applied Physics Letters, 82, 364-366.

Brown, R., 1928. Edinburgh New Phil. J.

Burns, M.A., Johnson, B.N., Brahmasandra, S.N., JamesK.H., Webster, R., Krishnan, M., Sammarco, T.S, Man, P.M., Jones, D., Heldsinger, D., Mastrangelo, C.H., and Burke, D.T., 1998. An Integrated Nanoliter DNA Analysis Device. Science, 282, 484-487.

Chambers, R.D., Holling, D., Spink, R.C.H., Sandford, G., 2001, Elemental fluorine - Part 13. Gas-liquid thin film microreactors for selective direct fluorination. Lab on Chip, 1, 132-137.

Cubaud, T., Ho, C.-M., 2004. Transport of bubbles in square microchannels. Physics of Fluids, 16, 4575-4585.

Cubaud, T., Ho, C.-M., 2004. Transport of bubbles in square microchannels. Physics of Fluids, 16, 4575-4585.

Cubaud, T., Tatineni, M., Zhong, X. and Ho, C.-M., 2005. Bubble dispenser in microfluidic devices. Physical Review E, 27, 037302.

Dietrich, N., Poncin, S., Li H.Z., 2007. Dynamique des bulles dans un micro-réacteur. Récents Progrès en Génie des Procédés, 95, isbn 2-910239-69-1, Ed. SFGP, Paris, France.

Dittrich, P.S., Manz, A., 2006. Lab-on-a-chip: microfluidics in drug discovery. Nature Reviews Drug Discovery, 5, 210–218.

Einstein, A., 1905. Ann. d. Physik 17, 549-560 (also demonstrated by Sutherland, W., 1905, Phil. Mag. 9, 781).

Fan, L.S., Yu, Z., Hemminger, O., 2007. Experiment and lattice Boltzmann simulation of two phase gas-liquid flows in microchannels. Chemical Engineering Science, 62, 7505-7514.

Frank, X., Dietrich, N., Wu, J., Barraud, R., Li, H.Z., 2007. Bubble nucleation and growth in fluids. Chemical Engineering Science, 62, 7090-7097.

Fries, D.M., Waelchli, S., Rudolf von Rohr, P., 2007. Gas-liquid two-phase flow in meandering microchannels. Chemical Engineering Journal, 135, S37-S45 .

Gañán-Calvo, A.M., 1998. Generation of steady liquid microthreads and micron-sized monodisperse sprays in gas streams. Physical Review Letters, 80 , 285-288.

Ganan-Calvo, A.M., Gordillo, J.M., 2001. Perfectly monodisperse microbubbling by capillary flow focusing. Physical Review Letters, 87, 274501.

Garstecki, P., Fuerstman, M.J., Stone, H.A., Whitesides, G.M., 2006. Formation of droplets and bubbles in a microfluidic T-junction – scaling and mechanism of break up. Lab on chip, 6, 437-446.

Garstecki, P., Stone, H.A., Whitesides, G.M., 2005. Mechanism for flowrate controlled breakup in confined geometries. Phys. Rev. Lett, 94, 164501.

Guillot, P., Colin, A., 2005. Stability of parallel flows in a microchannel after a T junction. Physical Review E, 72 (066301).

Haverkamp, V., Hessel, V., Lowe, H., Menges, G., Warnier, M. J. F., Rebrov, E. V.,de Croon, M. H. J. M., Schouten, J. C., Liauw, M. A., 2006. Hydrodynamics and Mixer-Induced Bubble Formation in Micro Bubble Columns with Single and Multiple-Channels. Chemical Engineering Technology, 29, 1015-1026.

Kobayashi, J., Mori, Y., Okamoto, K., Akiyama, R., Ueno, M., Kitamori, T., Kobayashi, S., 2004. A Microfluidic Device for Conducting Gas-Liquid-Solid Hydrogenation Reactions. Science, 304, 1305-1308.

Lindken, R., Westerweel, J., Wieneke, B., 2006. Stereoscopic micro particle image velocimetry. Experiments in Fluids, 11, 161-171.

Nisisako, T., Torii, T., Higuchi, T., 2002. Droplet formation in a microchannel network. Lab on a Chip, 2, 24-26.

Qu, W., Mudawar, I., 2002. Experimental and numerical study of pressure drop and heat transfer in a single-phase micro-channel heat sink. International Journal of Heat and Mass Transfer, 45, 2549-2565.

Thorsen, T., Roberts, W. R., Arnold, F. H., Quake, S. R., 2001. Dynamic pattern formation in a vesicle-generating microfluidic device. Physical Review Letters, 86, 4163-4166.

Thulasidas, T.C., Abraham, M.A., Cerro, R.L., 1997. Flow patterns in liquid slugs during bubble train flow in capillaries. Chemical Engineering Science, 52 , 2947-2962.

Tice, J. D., Song, H., Lyon, A. D., Ismagilov, R. F., 2003. Formation of droplets and mixing in multiphase microfluidics at low values of the Reynolds and the capillary number. Langmuir,19, 9127-9133.

van der Graaf, S., Nisisako, T., Schroe, C.G.P.H., van der Sman, R.G.M., Boom, R. M., 2006. Lattice Boltzmann Simulations of Droplet Formation in a T-Shaped Microchannel. Langmuir, 22, 4144-4152.

van Steijn, V., Kreutzer, M.T., Kleijn C.R., 2007. μ-PIV study of the formation of segmented flow in microfluidic T-junctions. Chemical Engineering Science, 62, 7505-7514.

Waelchli, S., von Rohr, R., 2006. Two-phase flow characteristics in gas-liquid micro reactors. International Journal of Multiphase Flow, 32, 791-806.

Wu, J., Lu, Z.Y., Hu, J.C., Feng, L., Huang, J.D., Gu, X.S., 2006. Disruption of granules by hydrodynamic force in internal circulation anaerobic reactors. Water Science and Technology, 54, 9-16.

Xiong, R., Bai, M., Chung, J.N., 2007. Formation of bubbles in a simple co-flowing micro-channel. Journal of Micromechanics and Microengineering, 17, 1002-1011.

Xu, J.H., Li, S.W., Wang, Y.J., Luo, G.S., 2006. Controllable gas-liquid phase flow patterns and monodisperse microbubbles in a microfluidic T-junction device. Applied Physics Letters, 88, 133506.

Yen, B.K.H., Gunther, A., Schmidt, M.A., Jensen, K.F., 2005. A microfabricated gas-liquid segmented flow reactor for high-temperature synthesis: The case of CdSe quantum dots. Angewandte Chemie International, 44, 5447-5451.

Zhang, H., Tumarkin, E., Peerani, R., Nie, Z., Sullan, R. M. A., Walker, G.C., Kumacheva, E., 2006. Microfluidic production of biopolymer microcapsules with controlled morphology. Journal of the American Chemical Society 128, 12205-12210.